Quantum mirages formed by coherent projection of electronic structure

H. C. Manoharan, C. P. Lutz & D. M. Eigler

IBM Research Division, Almaden Research Center, 650 Harry Road, San Jose, California 95120, USA

Image projection relies on classical wave mechanics and the use of natural or engineered structures such as lenses or resonant cavities. Well-known examples include the bending of light to create mirages in the atmosphere, and the focusing of sound by whispering galleries. However, the observation of analogous phenomena in condensed matter systems is a more recent development[1], facilitated by advances in nanofabrication. Here we report the projection of the electronic structure surrounding a magnetic Co atom to a remote location on the surface of a Cu crystal; electron partial waves scattered from the real Co atom are coherently refocused to form a spectral image or 'quantum mirage'. The focusing device is an elliptical quantum corral[2,3], assembled on the Cu surface. The corral acts as a quantum mechanical resonator, while the two-dimensional Cu surface-state electrons form the projection medium. When placed on the surface, Co atoms display a distinctive spectroscopic signature, known as the many-particle Kondo resonance[4–6], which arises from their magnetic moment. By positioning a Co atom at one focus of the ellipse, we detect a strong Kondo signature not only at the atom, but also at the empty focus. This behaviour contrasts with the usual spatially-decreasing response of an electron gas to a localized perturbation[7].

Experiments were performed with a scanning tunnelling microscope (STM) operating at 4 K in ultrahigh vacuum (UHV). The (111) surface of a single-crystal Cu sample was prepared by several cycles of Ar ion sputtering and UHV annealing, with surface cleanliness monitored by Auger spectroscopy. The sample was then cooled to 4 K and dosed with a calibrated Co electron-beam evaporator to typical coverages of ~13 atoms $(100\,\text{Å})^{-2}$ (0.007 monolayer). We use the convention that the voltage V across the STM tunnel junction is the sample bias with respect to the tip. As the STM tip, a polycrystalline Ir wire, was prepared through field emission followed by gentle collisions with the Cu sample, the exact chemical identity of the last atom terminating the tip was unknown. However, we have repeated the spectroscopy results given here with a tip terminated in an atom of known identity (Xe) to confirm that our results are independent of tip chemistry.

We demonstrate the existence of quantum mirages by using the Kondo resonance[4], a response which forms around individual magnetic moments on the metal surface. Although it was identified more than 30 years ago and studied extensively since then[8], the prototypical Kondo problem—namely, a single, well-characterized, magnetic impurity embedded in a non-magnetic host conductor—has eluded experimental access until quite recently, when STM spectroscopy was used to identify the Kondo resonance around single magnetic atoms placed on a non-magnetic metal surface[5,6]. The Kondo effect arises as a result of the exchange interaction between the localized magnetic moment of the impurity and the delocalized electrons in the metallic host. At sufficiently low temperatures T, nearby conduction electrons begin to align their spins to screen the spin on the local moment. A many-body spin-singlet state is thus formed, consisting of the local magnetic impurity surrounded by a spin compensation cloud of conduction electrons, such that no net moment remains at the Kondo site. This intriguing state has a special energy scale $k_B T_K$ associated with it, where T_K is the Kondo temperature (k_B is the Boltzmann constant). Only for $T < T_K$, and for certain combinations of magnetic atoms and host metals, is the Kondo effect expected to exist. As the constituent electrons in the Kondo screening cloud come predominantly from the Fermi surface of the metallic host, the Kondo effect may be observed spectroscopically as an acute perturbation or resonance in the renormalized density of states near the Fermi energy E_F. The spectral width of this resonance scales proportionally with T_K.

In Fig. 1 we present tunnelling spectra of Co atoms on Cu(111), in which the Kondo resonance is manifest as a sharp suppression in differential conductance dI/dV in the immediate vicinity of E_F ($V = 0$). As shown in Fig. 1a, this resonance is spatially centred precisely on the Co atoms and dies off over a lateral length scale of ~10 Å. The observed spectroscopic feature is quite narrow (9 mV full-width at half-maximum, FWHM) and very strong (the resonance magnitude is about 40% of the zero-bias conductance). The shift in the resonance minimum from $V = 0$ is not a measurement artifact and is determined to be about 1 mV. We observe nearly identical resonance features on all Co atoms encountered and with a variety of different STM tips.

Previously observed resonances associated with the Kondo effect over single magnetic atoms[5,6] have been interpreted in terms of Fano's model of interfering discrete and continuum channels[9]. We

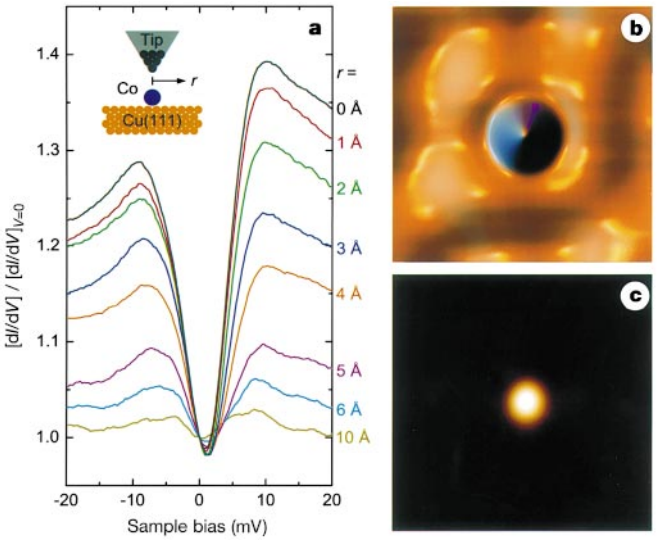

Figure 1 Detection of the Kondo resonance localized around a single Co atom on Cu(111). **a**, Tunnel spectra (normalized dI/dV) acquired over the Co atom for increasing lateral displacement r ($R_T = 100\,\text{MΩ}$ at $V = 10$ mV). Inset, measurement geometry. **b**, 35-Å square topograph ($V = 5$ mV, $I = 1$ nA) of an isolated Co atom (0.8-Å-high central bump) **c**, dI/dV map of the same area (average of $V = \pm 5$ mV acquisitions, $V_{a.c.} = 1$ mV r.m.s., $I = 1$ nA). Dark to light corresponds to increasing conductance. Examples of the three types of data obtained in this experiment: (1) Topograph images (**b**) were acquired with the scanning tunnelling microscope (STM) operating in constant d.c. current (I) mode, in which a closed feedback loop constantly adjusted tip height. (2) Tunnel spectra (**a**) were acquired by adding a small a.c. modulation $V_{a.c.}$ (1 mV r.m.s. at 201 Hz) to the d.c. bias V, opening the feedback loop (hence, holding the tip motionless with respect to the surface), and measuring dI/dV versus V through lock-in detection of the a.c. component of the tunnel current. Such spectra were essentially independent of the tunnel junction impedance R_T, determined by V/I before opening the feedback loop. (3) dI/dV image maps (**c**) were acquired simultaneously with associated topographs by applying an a.c. modulation (typically 250 μV to 1 mV r.m.s. at 201 or 1007 Hz) at a frequency exceeding the bandwidth of the feedback loop, and recording the lock-in detected dI/dV (conductance map) along with tip height (topograph) at fixed d.c. bias V while the tip was scanned in closed-loop constant-I mode. Both kinds of differential conductance measurements constitute a probe of the local density of states under the tip[17,18].

© 2000 Macmillan Magazines Ltd

find that our observed spectra can be fitted very well by a Fano line shape in the limit of small coupling to the discrete state ($q \ll 1$ in ref. 9); such fits reproduce the 'dip' structure along with the observed asymmetry and the shift in the minimum from $V = 0$. Following the theoretical results of ref. 6, the half width of the Fano resonance ($\Gamma/2$ in ref. 9) is taken to be equal to $k_B T_K$. Fits to our data from a large sampling of Co atoms on the Cu(111) surface yield $T_K = 53 \pm 5$ K.

The Cu(111) surface harbours a two-dimensional free electron gas. These electrons inhabit a surface state band which starts 450 mV below E_F. Co atoms placed on the surface are immersed in the two-dimensional electron sea. This fact is crucial to our results, as it is precisely these electrons that form the projection medium for the quantum mirage. In the topograph of Fig. 1b, the standing waves (equivalently, the energy-resolved Friedel oscillations) formed from the two-dimensional electrons scattering off a single Co atom are evident[10,11]. Weak variations in the Kondo resonance as a particular Co atom is moved along the surface correlate with the features in the underlying standing-wave field.

We are able to spatially map the Kondo screening cloud by simultaneously acquiring a dI/dV image while V is tuned to a small bias V_0 near the edge of the resonance ($|V_0|$ ranges from 5 to 10 mV for the measurements described). The presence of the Kondo resonance at a particular location on the surface removes spectral density between $V = 0$ and $V = V_0$ and, because the data is acquired in closed-loop constant-current mode, causes the tip to approach the sample and thus increases the measured dI/dV signal.

Figure 1c shows the dI/dV map associated with the single Co atom topograph in Fig. 1b. This visualization clearly reveals the location and extent of the Kondo resonance localized at the Co atom site.

We have used the discrete electronic states of elliptical quantum corrals[2,3] to project the mirage. As illustrated in Fig. 2a and b, an ellipse has the property that all classical paths emanating from one focus F_1 bounce specularly off the wall at arbitrary point P and converge on the second focus F_2. Furthermore, this path length (dashed line in Fig. 2a and b) remains fixed at $\overline{F_1PF_2} = 2a$ independent of the trajectory, where a is the semimajor axis length. Hence, if a scatterer is placed at one focus, all scattered waves will add with coherent phase at the other focus. We constructed a pair of resonators with the geometries sketched in Fig. 2a

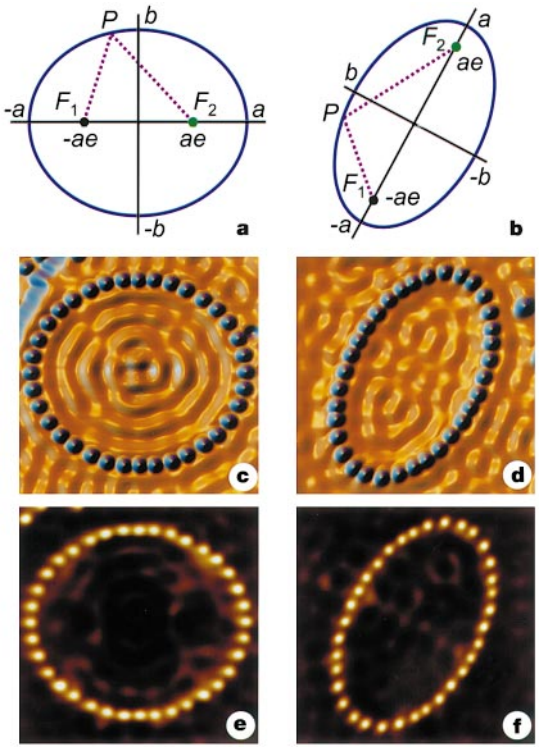

Figure 2 Elliptical electron resonators. **a**, Eccentricity $e = 1/2$; **b**, $e = 0.786$. **c**, **d**, Corresponding topographs of the experimental realizations ($a = 71.3$ Å for both ellipses) employing Co atoms to corral two-dimensional electrons on Cu(111). **e**, **f**, dI/dV maps acquired simultaneously with the corresponding topographs, tuned to image the Kondo resonance. ($V = 10$ mV, $V_{a.c.} = 250$ μV r.m.s., $I = 1$ nA for **c** and **e**; $V = 8$ mV, $V_{a.c.} = 1$ mV r.m.s., $I = 1$ nA for **d** and **f**). Image dimensions are 150 Å square and 154 Å square for the $e = 1/2$ and $e = 0.786$ ellipses, respectively.

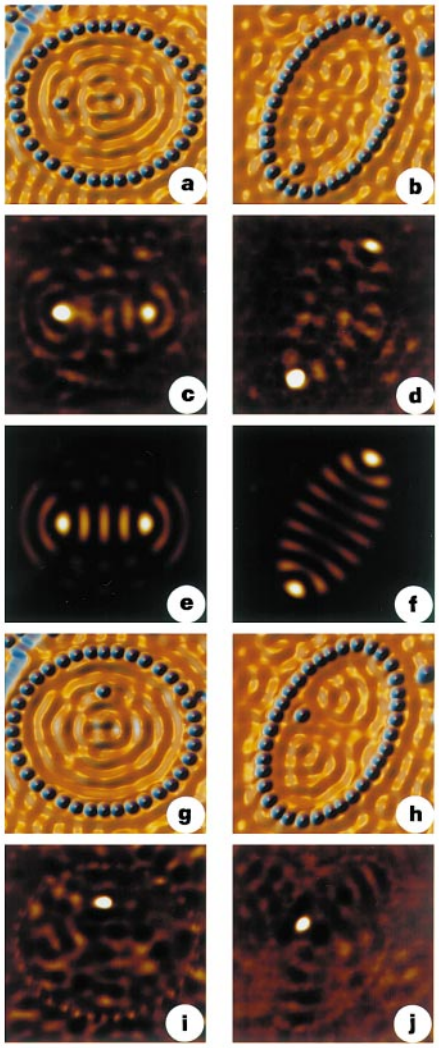

Figure 3 Visualization of the quantum mirage. **a**, **b**, Topographs showing the $e = 1/2$ (**a**) and $e = 0.786$ (**b**) ellipse each with a Co atom at the left focus. **c**, **d**, Associated dI/dV difference maps showing the Kondo effect projected to the empty right focus, resulting in a Co atom mirage. **e** and **f**, Calculated eigenmodes at E_F (magnitude of the wavefunction is plotted). When the interior Co atom is moved off focus (**g** and **h**, topographs), the mirage vanishes (**i** and **j**, corresponding dI/dV difference maps). Imaging conditions and dimensions as in Fig. 2. We have assembled over 20 elliptical resonators of varying size and eccentricity and searched for the formation of a quantum mirage. We find that as a is increased monotonically while e is fixed, the mirage is switched on and off. In each period of this switching, the classical path length $2a$ changes by a half Fermi wavelength. Because we also observe that two focal atoms, one on each focus, couple quite strongly with one another (as judged by the perturbation of the Kondo resonance) these oscillatory results may have a source akin to the RKKY (indirect exchange) interaction[19].

© 2000 Macmillan Magazines Ltd

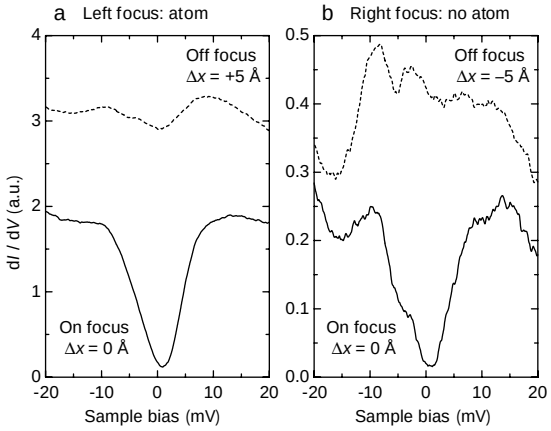

Figure 4 Tunnelling spectra. **a**, **b**, Near the left (**a**) and near the right (**b**) foci of the $e = 1/2$ elliptical resonator in the configuration depicted in Fig. 3a and c ($R_T = 100\,M\Omega$ at $V = 10\,mV$). Solid traces were acquired directly on focus; dashed traces were acquired with the tip displaced 5 Å off focus toward the centre of the ellipse. The electronic structure localized around the Co atom at the left focus is transmitted to the unoccupied right focus. (Note the axis scale change showing ~8 × signal attenuation. A background of constant slope has been subtracted from the data.)

and b by using the adatom sliding process[12,13] to position Co atoms to form the corral walls. STM topographs of the assembled resonators are shown in Fig. 2c and d, where the electron-confining effects are evident. The mean spacing between the Co atoms comprising the resonator walls is roughly four atomic sites on the underlying Cu(111) lattice, which has a nearest-neighbour spacing of 2.55 Å at $T = 4\,K$. This pair of ellipses was chosen to share the same $a = 71.3$ Å (hence the same focus-to-focus path length) but to have significantly different eccentricity $e = \sqrt{1 - b^2/a^2}$ (where b is the semiminor axis). The left and right columns of Fig. 2 pertain to $e = 1/2$ and $e = 0.786$ ellipses, which corral 84 and 56 electrons, respectively.

The associated dI/dV maps of the empty resonators are displayed in Fig. 2e and f. These maps show the Kondo resonance localized around each Co wall atom, but lack any significant Kondo signal within the ellipse. The faint interior features derive from the local density of states (LDOS) undulations of the ellipse eigenmodes closest to E_F. From these maps it is clear that the wall atoms themselves are not projecting the observed Kondo effect (Fig. 1a) into the confines of the resonator.

Next we studied the effects of placing a single Co atom at various locations inside each resonator. The results are summarized in Fig. 3. For a given geometry with an interior atom, we again acquired a simultaneous topograph and dI/dV map, and then subtracted the respective dI/dV map shown in Fig. 2e and f in order to remove the background electronic contribution of the standing wave LDOS and emphasize the Kondo component of the signal. The resulting dI/dV difference map was therefore tuned to spatially locate the Kondo signature of Co inside the resonator, while the associated topograph revealed the actual atom locations. The striking results of this measurement, shown in Fig. 3a–d, reveal two interior positions at which the Kondo resonance dominates for each ellipse: one signal is localized on the real Co atom at the left focus, while the other signal is centred on the empty right focus. In effect, a phantom (albeit weaker) copy of the Co atom has been created by projecting the localized electronic structure from the occupied focus to the unoccupied focus, thus creating the quantum mirage.

Since we are operating in a regime of reasonably large quantum numbers (~30–40), the most direct application of semiclassical concepts[14] such as classical foci, path lengths, s-wave scattering, and so on, can help explain some of the effects observed[15]. However, also visible in the dI/dV difference maps of Fig. 3c and d is reproducible fine structure throughout the interior of the resonators. Further insight into these observations comes from treating the system as strictly quantized. Calculations reveal that the additional features in the conductance maps correspond very well to the spatial structure of the eigenstate closest to E_F (approximating the elliptical boundary as a hard-wall box). The magnitude of the corresponding eigenstate for each ellipse is plotted in Fig. 3e and f. The quantum mirage is evidently projected predominantly through this state, which acts as a conduit between foci for the Kondo signature.

Modified geometries show that if the Co atom is placed at other positions within the ellipse besides one of the foci, even at high-symmetry points as shown in Fig. 3g and h, a corresponding mirage is not observed (see Fig. 3i and j).

The Kondo signature detected at the unoccupied focus (see Fig. 3c and d) exhibits about a third of the strength of that at the focal Co atom, while possessing comparable spatial extent. A component of this signal arises from the simple perturbation of the eigenmodes pictured in Fig. 3e and f, as their energies are shifted owing to an impurity inhabiting a region of high electron probability. For this reason, it is important also to examine standard open-loop tunnelling spectra acquired over the Co atom and its associated mirage.

In Fig. 4 we show the results of this test applied to the $e = 1/2$ ellipse. We have measured dI/dV near the left occupied focus (Fig. 4a) to compare with the corresponding spectra near the right unoccupied focus (Fig. 4b). The lower solid traces, obtained directly on focus, demonstrate that the mirage at the right focus is a surprisingly faithful spectroscopic replica of the real atom at the left focus: the resonance line shapes, widths, and zero-bias shifts are equivalent, and the Kondo signal is essentially only attenuated (by a factor of about eight). Moving off focus from either the real or phantom atom by the same distance (5 Å) toward the centre of the ellipse (upper dashed curves in Fig. 4) causes the detected Kondo signature to rapidly collapse, in agreement with the dI/dV difference image in Fig. 3c. These results provide perhaps the clearest demonstration that the electronic structure surrounding a focal Co atom is projected intact to the opposite focus.

We have confirmed that non-magnetic scatterers (sulphur and carbon monoxide) placed at one focus neither exhibit nor transmit a Kondo resonance to the opposite focus. We have also substituted non-magnetic carbon monoxide molecules for the Co wall atoms to verify that removing the Kondo effect along the wall does not influence the essential physics of the quantum mirage.

Some possible applications of the observed phenomena are evident. The elliptic geometry coupled with two-dimensional

© 2000 Macmillan Magazines Ltd

electrons could be employed to probe atoms and molecules remotely while minimizing the perturbing influences of a nearby local probe—these unwanted interactions might be chemical in nature or result from electric or magnetic fields emanating from an STM tip or other probe device. Our results also suggest altered geometries such as ellipsoids confining bulk electrons, or specially shaped electron mirrors (such as parabolic reflectors) electronically coupling two or more points. One might additionally envision performing other types of 'spectroscopy-at-a-distance' beyond electronic structure measurements, for example, detecting vibrational[16] or magnetic excitations.

We conclude with some remaining questions. Our calculations show that ellipses have a class of eigenmodes that possess strongly peaked probability amplitude near the classical foci (Fig. 3e and f are good examples). Our experiments reveal that the strongest mirages occur when one of these eigenmodes is at E_F and therefore at the energy of the Kondo resonance. When perturbed by a focal atom, this eigenmode still has substantial density surrounding both foci; it is therefore plausible that this quantum state 'samples' the Kondo resonance on the real atom and transmits that signal to the other focus. The physics behind this process is not completely understood. Also, given that a Kondo signature is detected at the empty focus, does this imply that a measurement there is simply providing us with a remote probe of the Co atom with the intervening two-dimensional electrons acting essentially like a wire? Or, as the Kondo effect on the Co atom requires a net spin polarization of the surrounding electron gas, does the projection of the Kondo resonance imply a modified spin polarization at the empty focus? We speculate that both interpretations are actually correct. Full answers to these questions, however, await further experimental and theoretical efforts.

Received 12 October; accepted 14 December 1999.

1. Spector, J., Stormer, H. L., Baldwin, K. W., Pfeiffer, L. N. & West, K. W. Electron focusing in two-dimensional systems by means of an electrostatic lens. *Appl. Phys. Lett.* **56,** 1290–1292 (1990).
2. Crommie, M. F., Lutz, C. P. & Eigler, D. M. Confinement of electrons to quantum corrals on a metal surface. *Science* **262,** 218–220 (1993).
3. Heremans, J. J., von Molnár, S., Awschalom, D. D. & Gossard, A. C. Ballistic electron focusing by elliptic reflecting barriers. *Appl. Phys. Lett.* **74,** 1281–1283 (1999).
4. Kondo, J. Resistance minimum in dilute magnetic alloys. *Prog. Theor. Phys.* **32,** 37–49 (1964).
5. Li, J., Schneider, W.-D., Berndt, R. & Delley, B. Kondo scattering observed at a single magnetic impurity. *Phys. Rev. Lett.* **80,** 2893–2896 (1998).
6. Madhavan, V., Chen, W., Jamneala, T., Crommie, M. F. & Wingreen, N. S. Tunnelling into a single magnetic atom: Spectroscopic evidence of the Kondo resonance. *Science* **280,** 567–569 (1998).
7. Kittel, C. *Quantum Theory of Solids* (Wiley, New York, 1963).
8. Hewson, A. C. *The Kondo Problem to Heavy Fermions* (Cambridge Univ. Press, Cambridge, 1997).
9. Fano, U. Effects of configuration interaction on intensities and phase shifts. *Phys. Rev.* **124,** 1866–1878 (1961).
10. Crommie, M. F., Lutz, C. P. & Eigler, D. M. Imaging standing waves in a two-dimensional electron gas. *Nature* **363,** 524–527 (1993).
11. Hasegawa, Y. & Avouris, P. Direct observation of standing wave formation at surface steps using scanning tunneling spectroscopy. *Phys. Rev. Lett.* **71,** 1071–1074 (1993).
12. Eigler, D. M. & Schweizer, E. K. Positioning single atoms with a scanning tunnelling microscope. *Nature* **344,** 524–526 (1990).
13. Stroscio, J. A. & Eigler, D. M. Atomic and molecular manipulation with the scanning tunneling microscope. *Science* **254,** 1319–1326 (1991).
14. Tomsovic, S. & Heller, E. J. Semiclassical construction of chaotic eigenstates. *Phys. Rev. Lett.* **70,** 1405–1408 (1993).
15. Chan, Y. S. & Heller, E. J. Scanning tunnel microscopy surface state electron scattering: Two-tip results from one-tip data. *Phys. Rev. Lett.* **78,** 2570–2572 (1997).
16. Stipe, B. C., Rezaei, M. A. & Ho, W. Single-molecule vibrational spectroscopy and microscopy. *Science* **280,** 1732–1735 (1998).
17. Lang, N. D. Spectroscopy of single atoms in the scanning tunneling microscope. *Phys. Rev. B* **34,** 5947–5950 (1986).
18. Everson, M. P., Jaklevic, R. C. & Shen, W. Measurement of the local density of states on a metal surface: Scanning tunneling spectroscopic imaging of Au(111). *J. Vac. Sci. Technol. A* **8,** 3662–3665 (1990).
19. Kittel, C. Indirect exchange interactions in metals. *Solid State Phys.* **22,** 1–26 (1968).

Acknowledgements

We thank B. A. Jones, E. J. Heller, J. S. Hersch, G. Fiete, A. J. Heinrich and C. T. Rettner for helpful discussions, and L. Folks for expert assistance with image preparation.

Correspondence and requests for materials should be addressed to H.C.M. (e-mail: hari@alumni.princeton.edu).

Experimental test of quantum nonlocality in three-photon Greenberger–Horne–Zeilinger entanglement

Jian-Wei Pan*, Dik Bouwmeester†, Matthew Daniell*, Harald Weinfurter‡ & Anton Zeilinger*

* *Institut für Experimentalphysik, Universität Wien, Boltzmanngasse 5, 1090 Wien, Austria*
† *Clarendon Laboratory, University of Oxford, Parks Road, Oxford OX1 3PU, UK*
‡ *Sektion Physik, Ludwig-Maximilians-Universität of München, Schellingstrasse 4/III, D-80799 München, Germany*

Bell's theorem[1] states that certain statistical correlations predicted by quantum physics for measurements on two-particle systems cannot be understood within a realistic picture based on local properties of each individual particle—even if the two particles are separated by large distances. Einstein, Podolsky and Rosen first recognized[2] the fundamental significance of these quantum correlations (termed 'entanglement' by Schrödinger[3]) and the

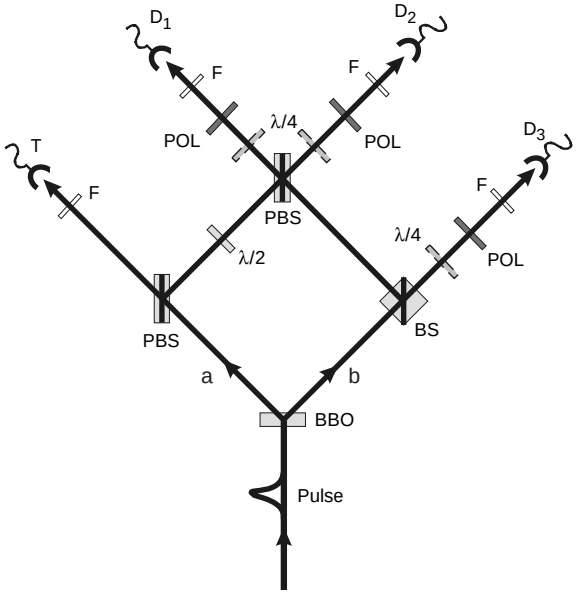

Figure 1 Experimental set-up for Greenberger–Horne–Zeilinger (GHZ) tests of quantum nonlocality. Pairs of polarization-entangled photons[28] (one photon *H* polarized and the other *V*) are generated by a short pulse of ultraviolet light (~ 200 fs, λ = 394 nm). Observation of the desired GHZ correlations requires fourfold coincidence and therefore two pairs[29]. The photon registered at T is always *H* and thus its partner in **b** must be *V*. The photon reflected at the polarizing beam-splitter (PBS) in arm **a** is always *V*, being turned into equal superposition of *V* and *H* by the λ/2 plate, and its partner in arm **b** must be *H*. Thus if all four detectors register at the same time, the two photons in D_1 and D_2 must either both have been *VV* and reflected by the last PBS or *HH* and transmitted. The photon at D_3 was therefore *H* or *V*, respectively. Both possibilities are made indistinguishable by having equal path lengths via **a** and **b** to D_1 (D_2) and by using narrow bandwidth filters ($F \approx 4$ nm) to stretch the coherence time to about 500 fs, substantially larger than the pulse length[30]. This effectively erases the prior correlation information and, owing to indistinguishability, the three photons registered at D_1, D_2 and D_3 exhibit the desired GHZ correlations predicted by the state of equation (1), where for simplicity we assume the polarizations at D_3 to be defined at right angles relative to the others. Polarizers oriented at 45° and λ/4 plates in front of the detectors allow measurement of linear *H′*/*V′* (circular *R*/*L*) polarization.

© 2000 Macmillan Magazines Ltd